INTERNATIONAL ATOMIC ENERGY AGENCY
UNITED NATIONS EDUCATIONAL, SCIENTIFIC AND CULTURAL ORGANIZATION
INTERNATIONAL CENTRE FOR THEORETICAL PHYSICS
I.C.T.P., P.O. BOX 586, 34100 TRIESTE, ITALY, CABLE CENTRATOM TRIESTE

H4.SMR/452-50

# ADRIATICO CONFERENCE ON FOURIER OPTICS AND HOLOGRAPHY

## *HOLOGRAPHY*

## *HOLOGRAPHIC INTERFEROMETRY*

Prof. Werner P. O. Jüptner

Bremen Institut Fur Angewandte

Bremen F.R. Germany

*HOLOGRAPHY*

*HOLOGRAPHIC INTERFEROMETRY*

Werner P.O.Jüptner

March 1990

C O N T E N T



*Holography and Holographic Interferometry*

Werner P.O. Jüptner, BIAS, Bremen, FRG

# 1. Introduction

## 1.1 General Remarks

Holography and its applications, especially holographic interferometry (HI), are fascinating parts of modern physics and engineering sciences. The main reason is the fact that holography is the two-dimensional coding of a three-dimensional information instead of the two-dimensional image of conventional photography or TV-cameras, fig. 1.1: By means of holography, the image of a three-dimensional object is stored with whole the depth information in a two-dimensional plane and the information is distributed over whole the plate. This means that holography is an ideal 3D-2D-converter, which is easy to be applied and has a good error redundancy.

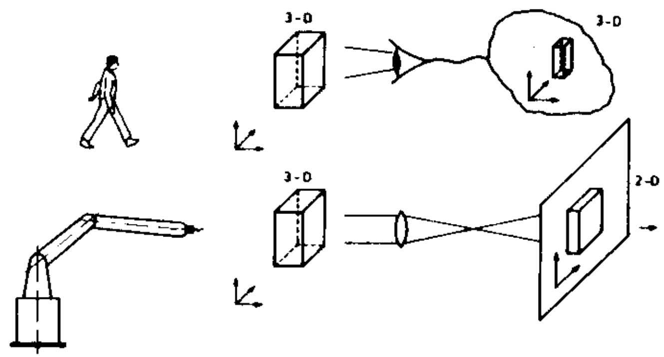


Fig. 1.1: Human and machine imaging

Holography may be applied to very different technical and artifical tasks. The potential of three-dimensional imaging leads to applications in advertisement and education: the fact of depth information is more related to human experience and gives more imagination than a two-dimensional picture. For artist a new tool is given, which starts to be used in unexperienced ways of viewing. In technical sciences holography becomes a tool as main part of optical computers, as holographic optical elements or as memory for interferometric applications.

Some of the applications of holography will be reviewed in the seminar. In this report the fundamentals of holography and holographic interferometry will be be the main subject.

## 1.2 Historical Remarks

Holography has some really old roots. In the beginning of the 19th century A.J.Fresnel (1788 - 1827) described the zone plate /1/, named after him, fig. 1.2: The zone plate is a system of black and white

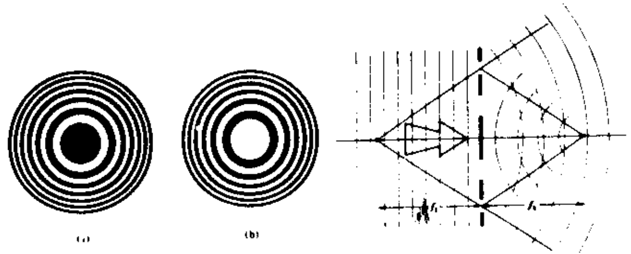

Fig. 1.2: Fresnel zone plate

rings. The radius of each ring is proportional to the square root of the ring number:

$$r_m \approx \sqrt{m} \qquad (1.2.1)$$

This leads to a grating with a changing grating constant, contrary to a standard grating, fig. 1.3. This leads to a changing diffraction,

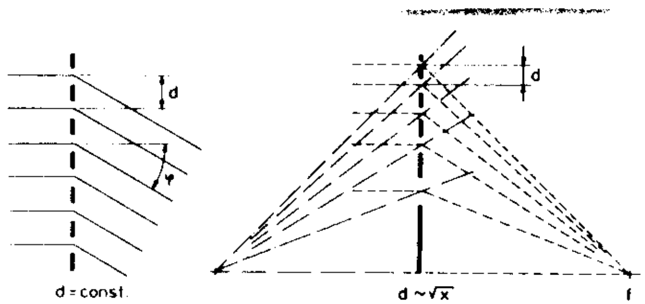


Fig._1.3: Grating and zone plate diffraction



especially an increasing diffraction, with the distance from the center of the zone plate. It can be derived by the laws of diffraction on a grating

$$\sin\varphi = n \lambda / d \qquad (1.2.2)$$

with $\varphi$ : diffraction angle for nth order
$n$ : order
$\lambda$ : wave length
$d$ : grating constant, difference between two slots

that a linear grating with slot distances proportional to the square root of the slot number diffracts a parallel light beam into three main parts: One part (the zero order) is only attenuated, one part (the first order) is diffracted into a point in the distance f from the grating and one part (the minus first order) seems to come out of a point in the distance -f on the light source side of the grating. Of course, the assumption of only three diffraction orders is valid for sinusoidal gratings, so the drawing might be thought to be binary image of such a grating. An easy procedure to get a Fresnel zone plate was mentioned by Lord Raleygh: One has to take two beams, e.g. a parallel one and a point source beam on the axis of the parallel beam. In a certain distance F from the point source a photo plate has to be placed, in the most simple case perpendicular to the beam axis. The lightened plate can be processed. then the amplitude distribution of transparency is like in a zone plate but sinusoidal - as long as the efficiency of the plate is proportional to the intensity. By the laws of the Fresnel zone plate, one can prove that for this plate is valid

$$(1/a + 1/b) = m \lambda / r_m^2 \qquad (1.2.3)$$

with $a = \infty$ : $b = f = F$ and $f = r_1^2 / (m \lambda)$

This leads directly to the principle of holography: The Fresnel zone plate produced with two beams as mentioned before is a hologram of one light point: If this light point is thought to be the object, it will be imaged by the second beam into the photo-sensitive plate. After illuminating the processed plate with the parallel beam, the virtual and a real image of the point source is reconstructed in the real positions: That is holography according to Gabor /2/. He suggested a comparable set-up to take a hologram from a slide with only few information in it, fig. 1.4.

However, the lack of this method is, that the the reference beam source, the virtual image and the real image are on one axis one behind the other. By this, the observation of the vitual image is difficult. Leith and Upatnieks therefore suggested to introduce an out-of-axis reference beam /3/. Additionally, there is no requirement to use a parallel reference beam. This leads to the common form of set-ups of today, fig. 1.5. In this case each surface point of the object might be thought to be a light point as mentioned before. Of course, this arises not any longer a simple zone plate, but a distribution of black and white spots and lines, difficult to understand.

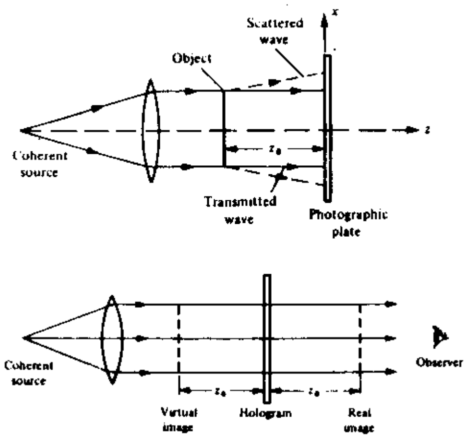


Fig. 1.4: In-line holography (Gabor)

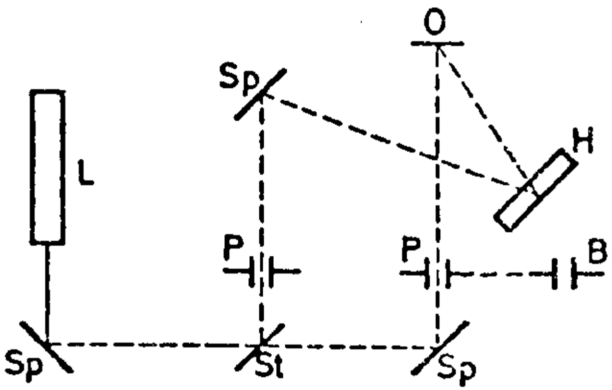


Fig. 1.5: Common set-up for holography





## 2.1 Holographic imaging

The basic idea of holographic imaging is to combine a the object wave carrying the information with a reference wave carrying no information (or a easy to reconstructed information) in order to store the phase information, fig. 2.1. These two waves interfere leading to a complex field of intensity distributions: Each object point can be thought to create a zone plate or a part of it. All these different zone plates - interacting with each other - are stored in the photo-sensitive medium. After processing the photo plate, the image is reconstructed with the reference wave only. The different images of the object points are reproduced in the way described in chap. 1.2 for one light source point and the two images of whole the object appears.

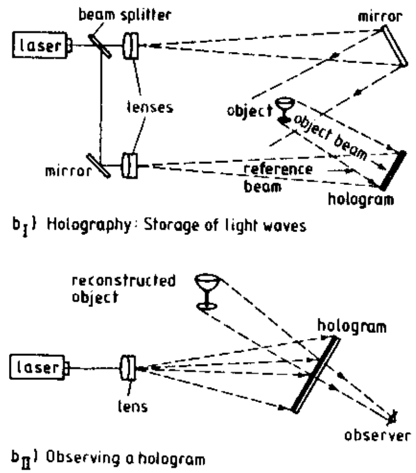


Fig. 2.1: Holographic imaging

The mathematical description of holography can be treated as follows: The object wave in the plane of the photo-sensitive plate may be expressed by

$$E_o = E_{oo} \exp[i\ (\omega t + \phi_o(x,y,z))] \qquad (2.1.1)$$

with $E_o$ : electrical vector of light wave from object
$E_{oo}$ : amplitude of the electrical vector
$\omega$ : circular frequency of the light wave
$\omega = 2\pi\nu$
$\phi$ : phase distribution of object light wave

This object wave interferes with a reference wave given by

$$E_R = E_{R0} \exp[i\ (\omega t + \phi\ (x,y,z))] \qquad (2.1.2)$$

with $E_R$ : electrical vector of reference light wave
$E_{R0}$ : amplitude of the electrical vector
$\omega$ : circular frequency of the light wave
$\omega = 2 \pi \nu$
$\phi_R$ : phase distribution of reference light wave

The frequency of the object and the reference wave are the same in order to get time-independent interferences. This is necessary for the imaging of the hologram. $\phi_R$ is usually a slidely varying function of x, y and z. The interference of the wave produces an intensity distribution given by

$$I = (E_O + E_R)\ (E_O + E_R)^* \qquad (2.1.3)$$

$$= E_{O0}{}^2 + E_{R0}{}^2 + E_{O0}\ E_{R0}{}^* \exp[i\ (\phi_O - \phi_R)]$$

$$+ E_{O0}{}^*\ E_{R0} \exp[-i\ (\phi_O - \phi_R)]$$

Equ.(2.1.3) describes a time-constant intensity distribution, which still carries the information of the object wave: the third and the fourth term on the right side indicate the dependency of the intensity on the two incident waves. This intensity distribution can be registered by any light sensitive medium with sufficient resolution, e.g. photographic plates. In generally the interference fringe spacing is in the order of some wavelength or less.

When the photographic plate is exposed to the intensity distribution according to equ.(2.1.3) and developed, the transmission can be assumed to be linearly dependent on the incident intensity with a factor β (even more complex ways of mathematical treatment lead a comparable result):

$$T = T_0 + \beta\ I \qquad (2.1.4)$$

The second step in holographic imaging is to illuminate the replaced hologram (= exposed and developed photographic plate) with the reference wave. Mathematically this means:

$$E_R\ T = E_R\ T_0 + E_R\ \beta\ E_{O0}{}^2 + E_R\ \beta\ E_{R0}{}^2 \qquad (2.1.5)$$

$$+ \beta\ E_{R0}\ E_{O0}\ E_{R0}{}^* \exp[i\ (\omega t + \phi_O)]$$

$$+ \beta\ E_{R0}\ E_{O0}{}^*\ E_{R0} \exp[i\ (\omega t - (\phi_O - 2\ \phi_R))]$$



$$E_R\ T = \alpha\ E_R \qquad \text{reference wave} \qquad (2.1.6)$$

$$+ \beta\ E_{R0}{}^2\ E_O \qquad \text{object wave}$$

$$+ \beta\ E_{R0}{}^2\ E_{O0}{}^* \exp[i\ (\omega t - \phi_O)]\ \exp(-2\ i\ \phi_R)] \qquad \text{real image wave}$$

with $\alpha = T_0 + \beta\ (E_{O0}{}^2 + E_{R0}{}^2)$

This equation describes three waves behind the hologram: the diffraction order zero results in the attenuated, incident reference wave, of course. The second term, related to the first diffraction order, describes the old object wave, only changed by a time and space constant factor. Additionally appears an object wave with a negative phase distribution. This is a real image of the object, but its position is modified by the phase factor $2\ \phi_R$, so the real and the virtual image are not in axis.

There are a lot of different results out of the before mentioned equations that can be discussed. Some of them are related to optical computing and discussed in the special lecture on this topic. Another interesting application is the on-line image enhancement by filtering with the inverse transfer function. The main topic of this lecture, holographic interferometry, uses only the full reconstruction of the object wave with all details in order to compare one state of an object with a slidely changed one. This will be discussed in the following chapters.

## 2.2 Types of Holograms

In the chap. 1.2 and 2.2 the Gabor in-line and the usual Leith-Upatnieks off-axis holograms have been mentioned. There are a few other types of taking holograms which will be described for example.

### Fourier transform hologram

The object is illuminated with nearly parallel light, fig. 2.2. Additionally, the reference beam is focused in a way, that it seems to come from a source point in the object plane near the object. This results in low spatial interference fringe frequencies. There is only one disadvantage: the condition of sufficient spacing of the interference fringes is only valid for a small region in depth. This limits the application to small objects in well-known position.

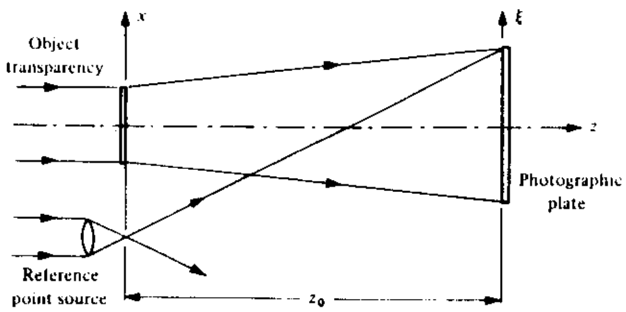


Fig. 2.2: Fourier transform hologram /4/

Image plane hologram

An arrangement, comparable to the ESPI (Electronic Speckle Pattern Interferometry) set-up /5/, is the image plane hologram, fig. 2.3: The object is illuminated with laser light and then imaged onto the photo plate or a camera target /6/, fig. 2.4. Additionally, a nearly parallel reference beam is given parallel to the object beam onto the target and an aperture limits the spatial frequencies of the object image. So, the interference fringe spacing is suitable to the resolution of TV camera targets. The advantage of the technique is the fast storage of the hologram and the high stability against environmental disturbances. However, the noise increases with smaller apertures by creating larger speckles, fig. 2.5. This method can be used for interferometric measurements, known as ESPI, a method which is starting to get more applied by the work of J.Tyrer, UK, and O.Løkberg, Norway.

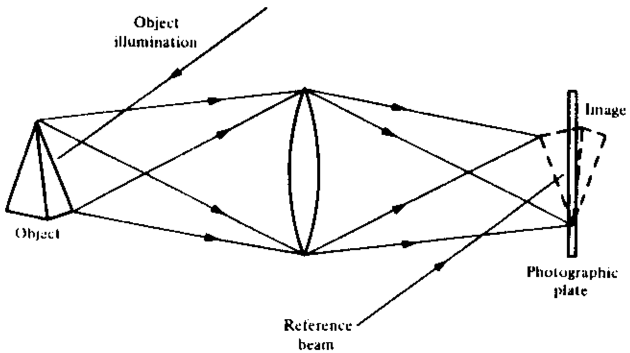


Fig. 2.3: Image plane hologram /4/



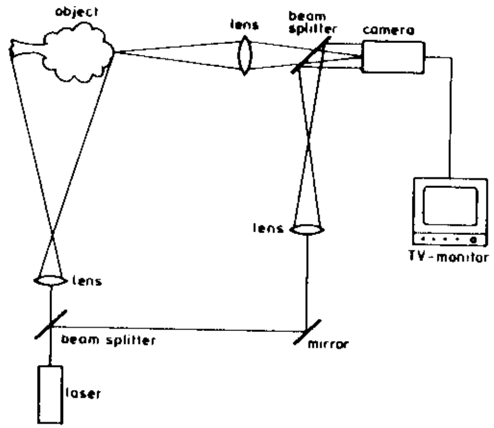


Fig. 2.4: TV hologram camera /6/

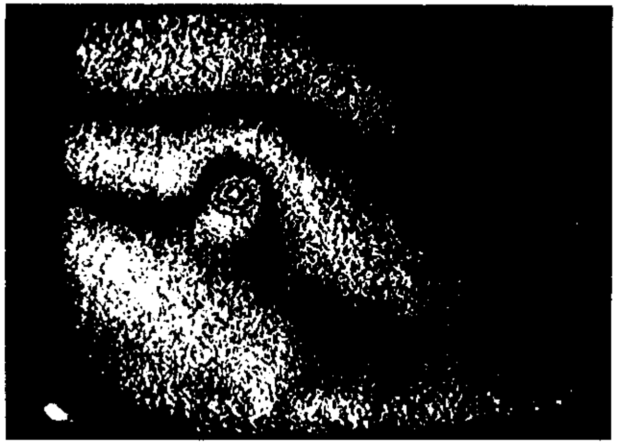

Fig. 2.5: TV hologram tire testing /6/

## 2.3 Holographic Materials

Different physical and practical requirements determine the choice of the holographic storing material:

- It should match the wavelength of the laser.
- It should be sensitive.
- It should be easy and fast to be processed.
- It should be reusable.
- It should have a high resolution.

Unfortunately, not all of the before mentioned qualities are available in one and the same material. So in practice one has to decide with regard to the special application which material is the best fit. A list of the available materials is given in table 2.4.1. Additionally, the qualities of the common photographic films and plates are given in table 2.4.2.

## 2.4 Remarks on the Variety of Holograms and Holographic Applications

Holography spreads into a lot of applications.

The variety starts with the acquisition of a hologram: Usually we think to store the hologram with a photographic plate. Of course, there is a chance to do this directly on the target of a video camera. This leads to the TV-holography and/or to the ESPI, which are closely related. As long as this is holographic interferometry, this should be treated as a part of the usual holographic interferometry with special requirements.

Holography has a large effect in demonstrating three-dimensional objects. By this it can be a tool for education or advertising. This is a lesson of it's own.

Furthermore, there are really new moments in arts with this new technique. But again, this will a special lesson. A good address to people interested in this field might be the New York Museum of Holography or the Lauk Museum of Holography in Cologne.



# 3. Holographic Interferometry

## 3.1 Fundamentals of Holographic Interferometry

The reconstructed hologram contents all information about the imaged object. If it is combined with another image of the same object, which suffered small changes by dislocation, deformation etc., the two images interfere, fig 3.1. If the object has a rough surface each

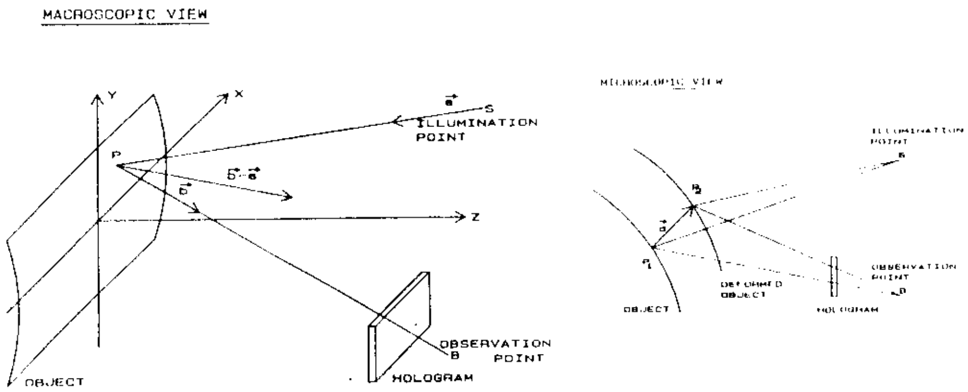


Fig. 3.1: Holographic interferometry

point of the surface can be treated separately. According to Stetson each change of the light way from the source over the object point to the observation point by a wavelength produces one change in intensity from black to white and back or vice versa /1/. This means one interference fringe appears. The change of the light way is given by the scalar product of the geometrical dislocation of the object point and the sensitivity vector:

$$n \lambda = \boldsymbol{\nu}\, d \qquad (3.1.1)$$

with $n$ : order of the fringe
$\lambda$ : wavelength of the laser
$\boldsymbol{\nu}$ : sensitivity vector
$d$ : dislocation vector of the object point

The sensitivity vector is the vector difference of unity vector from the ligth source to the object point and the unity vector from the object to the observation point:

$$\boldsymbol{\nu} = s \quad b \qquad (3.1.2)$$

## 3.2 Set-Up for Holographic Interferometry

### *3.2.1 Set-up*

The basic set-up is shown in fig. 3.2. The laser light, coming from the laser L, is splitted by a beam splitter St into two parts:

- the reference beam runs from the focussing lens $L_1$ with the pin hole $P_1$ and the mirror $Sp_1$ to the hologram H;
- the object beam runs over the mirror Sp and the lens $L_2$ with the pinhole P to the object O, from there the light is scattered to the hologram H.

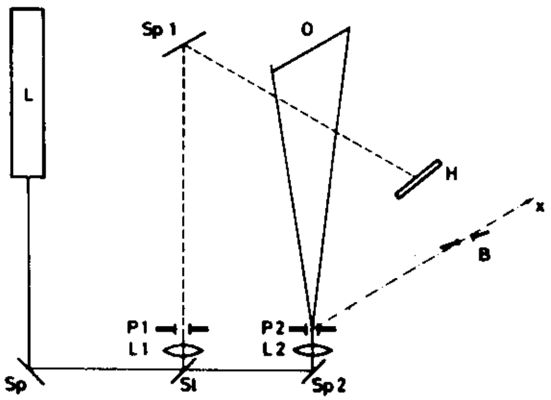


Fig. 3.2: Set-up for holographic interferometry, schematic

The observation point B is behind the hologram. This point defines with the source point P the fringe appearence, the snesitivity of the set-up and the evaluation, demonstrated by the axis *x*. The position of the hologram has a poor influence on the holographic interferometry.

The shown set-up consist two holograms and two observation points. This shall demonstrate that for quantitative evaluation more than one interferogram is needed with different sensitivity vectors and one can combine these set-ups in an easy way.



### *3.2.2 Optimization of the set-up sensitivity*

The basic equation

$$n \lambda = \nu d \qquad (3.1.1)$$

demonstrates that the number of fringes depends on two factors. One is the dislocation of the surface point and is only ruled by the object. the second is the sensitivity vector, which is mainly ruled by the set-up and the position of the object in the set-up. In order to optimize the set-up for the dislocations to be measured one can define geometric functions as the components of the sensitivity vector in three specific directions. An adequate coordinate system is defined by the following, fig. 3.3: The x-axis runs in the direction from the light source to the observation point. The origin of the coordinate system is at half the distance between these two points. The y-axis is in the plane from the origin to the object and the z-axis is given by the requirements of carthesian coordinates. Furthermore the coordinates shall be normalized by the half-distance between source and observation point $x_f$:

$$\eta = x / x_f \quad ; \quad \mu = y / x_f \quad ; \quad \zeta = z / x_f \qquad (3.2.1)$$

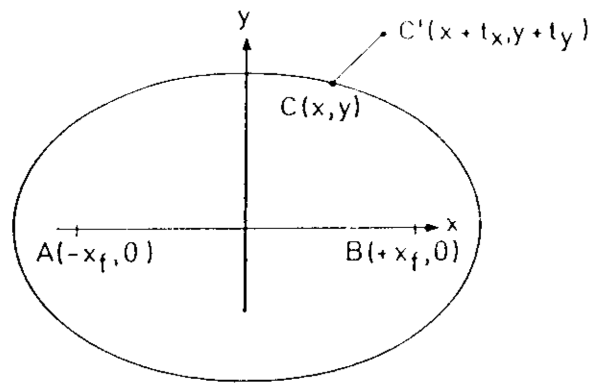


Fig. 3.3: Definition of coordinate system

The basic equation can be written as

$$n \lambda = \nu\ d + \nu\ d + \nu\ d \qquad (3.2.2)$$

$$\text{with } \nu = (x - x) / SQRM + (x + x) / SQRP \qquad (3.2.3)$$

$$\nu = y / SQRM + y / SQRP$$

$$\nu = z / SQRM + z / SQRP$$

$$SQRM = \sqrt{(x - x)^2 + y^2 + z^2}$$

$$SQRP = \sqrt{(x + x)^2 + y^2 + z^2}$$

The sensitivity of the set-up for different dislocations or deformations can be shown in diagrams for the geometric functions, fig. 3.4.

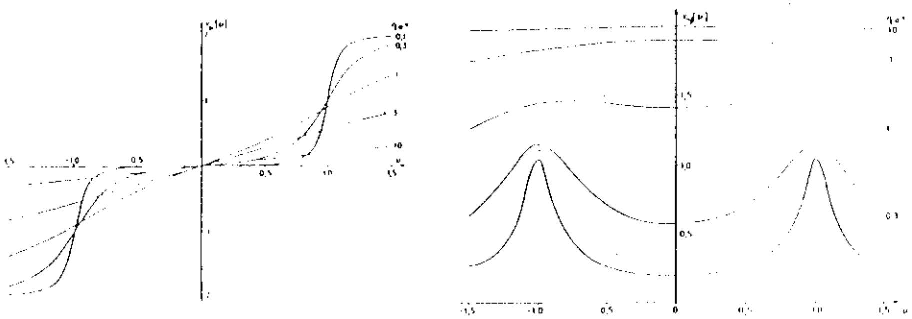

Fig. 3.4: Geometric function for x- and y-dislocation



### 3.3 Remarks on Interferogram Types

The most common types of interferograms are:

*Real time*

The first state of the object is imaged by a hologram. The changed object is observed through the reconstructed hologram, this means both the object and the reference beam stay unchanged.

Advantage: - The change of the object can be observed during the time of change. Dynamic loadingscan be filmed.
- Phase shift evaluation can be applied easily.

Disadvantage: - Usually it is difficult to get the best contrast.
- The documentation is not inherent in the measurement.
- Any unallowed change of the object destroys the measurement.

*Double exposure*

Both states of the object are stored in a hologram, usually in the same one. The reconstruction is done with only the reference beam.

Advantage: - Inherent documentation, even when the hologram breaks.
- Easy set-up, adequate to pulsed holography.
- Easy change of reference wave.

Disadvantage: - No dynamic observation possible.
- Phase shift evaluation is more difficult to apply.

*Time average*

The state of the object is changed during the time of hologram exposure. The reconstruction is done only with the reference beam. This method is favorately used for vibration analysis.

Advantage: - Easy set-up.
- Easy evaluation.

Disadvantage: - Only adequate to vibration analysis.
- Amplitude of deformation is strongly limited.

/1/ Powell, R.L.; Stetson, K.A.; "Interferometric Vibration Analysis by Wavefront Reconstructions", J.Opt.Soc.Am. 55,1593-1598 (1965)

## 4. Evaluation of Interferograms

In chap. 3 the theory of the holographic interferometry was described. It was shown that the calculation of the fringe system and the fringe order can be done easily when the displacement and the set-up are known. More difficulties arise when the inverse problem has to be handled that means to evaluate one or more interferograms in order to estimate an unknown displacement. The main problem in this case is to determine the fringe order as a function of the coordinate. For quantitative evaluation by a computer this are two problems in practice: to determine the absolute fringe order and to do this automatically. There are several approaches to solve the problem. The most common will be reported in the next chapters.

### 4.1 Basic Problem

The quantitative evaluation of the fringe system and of the HNDT has to be done by a computer. The first step is to evaluate the interference phase because the interference phase is strongly related to the dislocation by the multiplication with the sensitivity vector. The problem to evaluate the coordinate/fringe-order relation is to determine the phase at a given point automatically. The first attempt is to measuere the intensity I and to solve a function like

$$I = I_0 \cos\varphi + I_1 \qquad (4.1.1)$$

with $I$ : measured intensity
$I_0$ : amplitude of interference (unknown)
$I_1$ : ground intensity (unknown)
$\varphi$ : interference phase (to be evaluated)

were not successful even if sophisticated image analysis procedures were applied. One of the best is an approach by Crostack /1/ to fit the data of neighbourhood points by a locally matched cos-function with sliding frequencies. The reason for the difficulties is the composition of the intensity from different contributions, fig. 4.1.1:

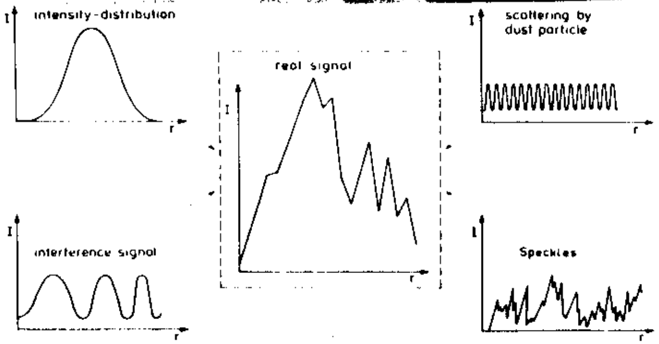


Fig. 4.1.1: Contributing signals to measured intensity



- The basic intensity distribution is not flat. By illumination with a $TEM_{00}$ laser beam the distribution is something like a part of a Gaussian distribution.
- Diffraction effects, scattering etc. by the optics and dust particles in the beam path produce unestimable interference patterns. Computers - even with very sophisticated software - can hardly decide between this noise and the real information.
- The coherent noise called speckles produces an additional pattern, which has minima and maxima, regardless of the real information.
- Last not least, the information pattern gives a contribution.

There are different methods to evaluate the phase distribution: One of the most accurate methods is the electronic phase measurement by the heterodyne technique /2/. This method was used for some very precise measurements but for practice it is to complicated. The standard method today is the phase shifting method, introduced in order to estimate residual stresses by holographic interferometry /3, 4/. The method is convenient for real-time holographic interferometry. It can be used in pulsed double-exposure holography, when two reference beams can be applied. This few remarks point out the difficulties of the phase shift method, although the accuracy is comparable to the heterodyne technique. A new method is the Fourier Transform Evaluation FTE /5/. This method is based on a unsymmetrical filtering in the Fourier plane. The back transformation delivers komplex values for the intensities at each point, which allow to calculate the phase at this point. The accuracy is less high than with the other methods but sufficient in most cases.

## 4.2 Visual Inspection and Evaluation

The easiest way to evaluate a fringe system is to measuere the locations of the minima and the maxima and to note this as a function of the coordinates. Then one can give this into a computer and form a fringe-order/location function. In most of the cases a least square fit can give a good correction of the data and a high accuracy is obtained. However, this will not match the requirements of a modern, automated evaluation. Even more, in the case of small inhomogenities, e.g. caused by defects, the method can disturb the needed result. So this method might be considered as a personal inspection and is mainly adequate to visual NDT.

*Accuracy*

The accuracy in quantitative evaluation is poor, since the estimation of the fringe order can be guessed with an accuracy of a quarter of a fringe. The safety in finding small deviations of the fringe system caused by flaws in the component is high, because a human eye can detect such effects much better than a computer today.

*Remarks*

Advantages:
- No investment needed for image processing.
- Good for visual inspection.

Disadvantages:
- Poor accuracy in quantitative evaluation.
- Time-consuming and expensive for human labour.
- Human errors will appear.
- Automated processing result needs human input into the computer.



## 4.3 Heterodyne Technique

The basic idea of the heterodyne technique is to introduce a frequency shift between the two waves forming the interferogram /2/, fig.4.3.1.

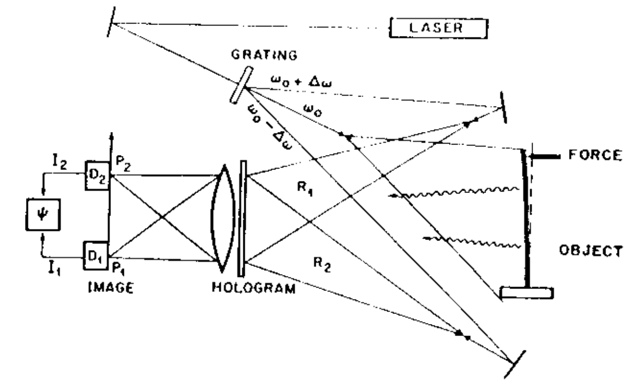


Fig. 4.3.1: Set-up for heterodyne phase measurement, schematic

The figure shows the experimental set-up for holographic interferometry with opto-electronic fringe interpolation. $R_1$ and $R_2$ are the two reference waves for independent recording of the two object states. $D_1$ and $D_2$ are photodetectors at the points $P_1$ and $P_2$, respectively, in the image plane of the object. The phase difference is measured with an electronic phasemeter. By this method it is possible to determine the phase at a given point relatively to a reference point. For whole the surface one has to fix one detector on a reference point (or his image) and to move the second detector over the surface of the object.

*Accuracy*

The accuracy depends on the speckle noise of the fringe pattern and on the electronic noise of the evaluation system. Usually this noise limits the phase measurement accuracy to 1/100 to 1/1000 of the wavelength.

*Remarks*

Advantage:
- High accuracy

Disadvantages:
- No industrial system available.
- Usually heterodyning is an off line technique.
- The Method is time-consuming by mechanical shift of sensor.

## 4.4 Phase Shift Technique

The problem to evaluate the fringe system automatically arises from the different contributions to the intensity of a given point:

- the object illumination and the reference wave have a non-flat basic intensity distribution,
- diffraction effects produce a interference system without the expected, but disturbing information,
- the coherent noise of the speckles is added randomly,
- the information pattern gives a contribution.

Normally it is very difficult for a computer to recognize the correct fringe pattern, if only the intensity at one point is measured. More adequate could be a video-based techniques: the phase shift method with an image analysis system /4/. The basic idea is given by the following: The reference wave of a real time reconstruction is shifted during the observation of the imaged object. This shift influences only the last of the before mentioned effects contributing to the real intensity of an interferogramm. so only the information pattern is changed by the phase shift. If this is done two or three times - this means three or four fringe systems are recorded - with the same shift angle, for each point of the fringe system three or four intensities are measured. By a solvable equation system the interference phase at this point can be calculated:

$$I = I \cos(\varphi + k\,\phi) + I \qquad k = 1,\dots,4 \qquad (4.4.1)$$

The solution of this as follows:

$$\cos(\phi) = \frac{I(x) - I(x) + I(x) - I_4(x)}{2\,I(x) - 2\,I(x)} \qquad (4.4.2)$$

$$\varphi = \arctan \frac{(I - I) + (I - I)\cos\phi + (I - I)\cos(2\phi)}{(I - I)\sin\phi + (I - I)\sin(2\phi)} \qquad (4.4.3)$$

It can be shown that the four image system with an arbitrary shift angle has a lot of advantages in practice. One of these is the redundancy against vibrations.

### *Accuracy*

The accuracy of the phase shift method is basicly the same as with heterodyning, 0.01 to 0.001 of the wavelength. Usually, the electronic noise of the used video system limits the accuracy to 1/100 of the wave-length.

### *Remarks*

Advantages:
- High speed, high accuracy and simple evaluation.
- Inherent two-dimensional evalution.

Disadvantages:
- Special set-up for the phase shifting needed.



## 4.5 Quantitative Evaluation by FTE

A new method is the Fourier-Transform-Evaluation (FTE). The method is based on a double Fourier transformation with an unsymmetrical filtering between the first and the second transformation /5/. The FTE is expected to have an accuracy of about a thirtieth of the wavelength, evaluation does not require any preparation - even photos of former experiments can be evaluated - and the method is stable against noise.

The intensity distribution of any interferogram can be written as:

$$I(x,y) = a(x,y) + b(x,y) * \cos(\Theta(x,y)) \qquad (4.5.1)$$

with
- $I(x,y)$: Measured intensity at the point $(x,y)$
- $a(x,y)$: Additive noise at the point $(x,y)$
- $b(x,y)$: Multiplicative noise at the point $(x,y)$
- $\Theta(x,y)$: Phase at the point $(x,y)$

The additive noise term contains e.g. scattering from dust particles; the multiplicative term e.g. the illumination distribution and the contrast of the interferogram. The phase distribution can be written:

$$\Theta(x,y) = 2\Pi/\lambda \; t \cdot s \qquad (4.5.2)$$

with
- $\lambda$ : Wavelength of the light
- $t$ : Dislocation of the point $(x,y)$
- $s$ : Sensitivity vector

The equation (4.5.1) can be written in the following way, according to Eulers formulas:

$$I(x,y) = a(x,y) + c(x,y) + c^{*}(x,y) \qquad (4.5.3)$$

with $c(x,y) = 0.5 * b(x,y) * \exp(\Theta(x,y))$

Although the intensity in this formula is given by the sum of two complex quantities, it remains a real-valued distribution. The intensity distribution, which is observed with a video camera, analog-to-digital converted and stored in the memory of a computer, can be transformed by a FFT program or hardware processor:

$$I'(u,v) = A'(u,v) + C'(u,v) + C'^{*}(u,v) \qquad (4.5.4)$$

This equation describes a symmetrical distribution in the Fourier plane because a real-valued function has a symmetrical Fourier transform distribution. The spectral distribution is filtered with a bandpass for one half of the Fourier plane except the point (0,0):

$$I'(u,v) = C'(u,v) \qquad (4.5.5)$$

The back transformation leads to a complex-valued intensity distribution, according to equ.(4.5.3) and (4.5.4). This rises the opportunity to calculate directly the phase by well-know mathematical operations:

$$I(x,y) = c(x,y) \qquad (4.5.6)$$

$$\Phi(x,y) = \arctan(Im(c(x,y))/Re(c(x,y))) \qquad (4.5.7)$$

An example for this evaluation in the one dimensional case is the shown simulation, fig.1. The intensity distribution is disturbed by a

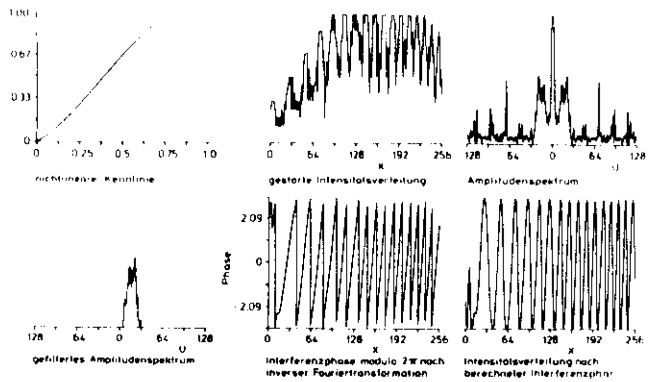


Fig. 4.5.1: Fourier Transform Evalution, simulation

non-flat back-ground intensity distribution, by a non-linear amplification, by a 4-bit analog/digital-conversion and by random noise, fig.1a. The Fourier transformation leads to a symmetrical function with high frequencies caused by the noise, fig.1b. A bandpass, which is mainly a half space filter but cuts also the high frequencies in this case, rises a unsymmetrical curve, fig.1c, which back-transformed and treated in the before-mentioned way results in the wanted phase distribution, fig.1d. The reconstructed intensity distribution demonstrates the quality of the filtering process, fig.1e.

*Accuracy*

The accuracy is under investigation today. First results predict an accuracy of about 0.01 of the wavelength.

*Remarks*

Advantages:
- Method can be applied to every interferogram, even those on photos.
- Only small computers with Fourier transform soft- or hardware is needed.

Disadvantages:
- Commercial systems under development.
- Best results in interactive mode.



## 5. Applications of Holographic Interferometry

### 5.1 Holographic Non-destructive Testing

Each NDT method consists three basic elements, fig. 5.1:

- The sender (emitter) puts any energy into the test object. The energy can be in the form of ultrasonics in US-testing, heat in thermography etc. In holographic NDT in most cases a mechanical or thermal load is applied, introducing deformation energy into the specimen.

- The test object transfers the energy to another surface or back to the input surface. The transfer of the energy - the attenuation, the scattering, the transformation or else - depends on the material properties and on the geometry of the specimen.

- The receiver records the transferred energy and converts it into a detectable signal.

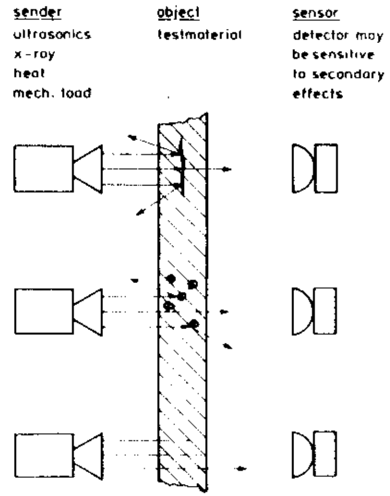


Fig. 5.1: Basics of NDT

Before starting the non-destructive testing of a given object the influence of the change of material properties to be detected on the energy transfer must be known from research and development work. In the special case of holografic NDT the load must be chosen adequate to the problem. Beside the operational load one can use thermal load or a change of the environmental pressure.

### 5.1.1 Loading

*Thermal load*

A useful loading of the test component is the thermal load. This can be done in different ways:

If the component excist fully or partially of metal, a direct heating can be applied by a current through the metal. The effect to be seen is the following: In the area of the flaw the heat transfer changes. By this an inhomogenous temperature field is induced which results in strain inhomogenities. These inhomogenities can be detected even through layers of several milimeters of steel.

If the material is a composite whether of metal-plastic or of fiber reinforced plastics the heat input can be acchieved by a (infrared) radiation. For metal layers at the surface the flux must not necessarily be uniform: Inside the metal the temperature field equalizes after a short distance (< 1 mm). For testing plastics the flux should be uni-form. Because of the bad heat conduction the heat input inhomogenities can be detected even after long distances (> 10 mm).

*Pressure load*

A usual loading of components is the pressure load. The component is given into a chamber or another environment, where the pressure may be lowered. With the lower pressure outside, the gas in the defects deforme the material around the defects. This can be detected. The pressure difference in common applications is up to 10 - 50 mbar. So one may think even to lower the pressure in whole rooms.

*Operational load*

The operational load can differ in a large variety of different types. So it is impossible to mention out all these as an example. But one fact can be stated: Usually, the testing load can be much smaller than the real one. Typically 10 % of the real load has to be applied.

### 5.1.2 Materials and Components

The holographic NDT can be applied to all materials and components. But in fact, conventional methods compete with the HNDT by their less expensive equipment and the easy way of evaluation in most cases. So HNDT is in general powerful for testing composite materials or structured components, not to be tested conventionally.



### 5.1.3 Honeycomb Test

The two-dimensional evaluation was applied to the deformation measurement of a radio antenna component during a non-destructive test. The object to be tested has a complicated structure. The cernel is build of a aluminium honeycomb. On both sides a bonding layer and a CRP-layer is added. The best loading for the HNDT was determined by first experiments with different loads like lower pressure, radiation heating and direct current heat.

The set-up was a symmetrical one with the sensitivity vector perpendicular to the surface of the component. The absolute value of the sensitivity vector was nearly 2. The interferograms were made in real-time technique, fig. 5.2. The filtering with two different half-space bandpasses enabled the calculation of whole the phase distribution, fig. 5.3. The evaluation lead to good results over nearly the

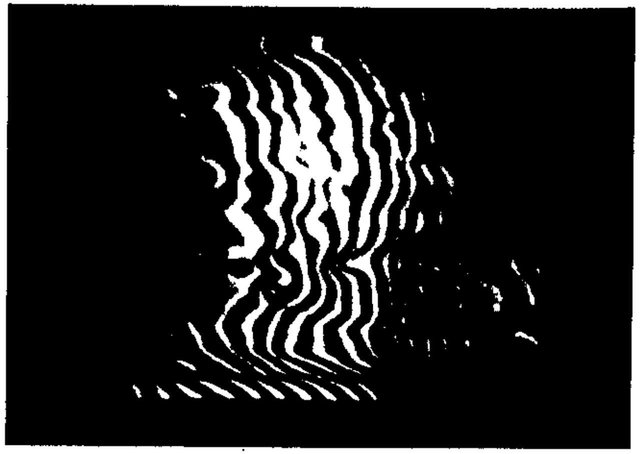

Fig. 5.2: Interferogram of a honey-comb structure test

whole surface. Only in the very dark parts of the object the evaluation made some difficulties. But by transforming the background and subtracting the background spectrum before the filtering even in this part the interferogram could be evaluated. Additionally, the deviation of the surface deformation was calculated. The main result of this quantitative evaluation is the additional information available from the same interferogram:

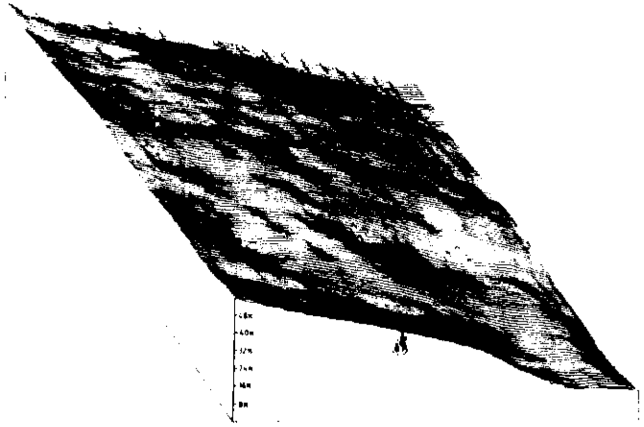

Fig. 5.3: Evaluation of the interferogram 5.2

- Big areas show the deformation inhomogenity of disbonds as they were expected by the preparation of the specimen.
- There is an additional structure in one direction which is due to the way of overall preparation of the bonding.
- Surprising was the evaluation of the small periodic structure which is mainly influenced by the thin layer between the honeycomb cernel and the CFRP-layer.

This demonstrates, that quantitative evaluation can show more of the internal structure of an object than one might expect. However, the evaluation had been done by visual inspection.



## 5.2 Construction Optimization of an Antenna Panel

In order to explore the very far universe, large radio-astronomic antennae are build up. One of this radio telescopes is mounted by the IRAM, institute for radio astronomic measurements, france. Because the task was to reach objects in a distance of more than 10 billion light years, the quality and stability demands were high. So, the contour should stay within a accuracy of better than 50 um under all loads, e.g. wind, temperature and gravity. To meet this requirements the whole antenna with a diameter of 30 m was constructed of smaller panels, size up to $1\ m^2$, fig. 5.4, which could be adjusted by piezo driven elements. But each of this smaller panels itself had to be stiff enough for the task. So different constructions of these panels were build up and had to be tested. The only tool powerful enough, was the holografic interferometry. A special interferometer was build up. With this interferometer it was possible to turn whole the set-up 90 for the gravity measurement. The fringe system, was evaluated by measuring the fringe order/location data manually. Afterwards these pairs of data were given into the computer. This is a simple method but it gave the necessary results. The tested panel shows large deformations, fig. 5.5. So it was changed.

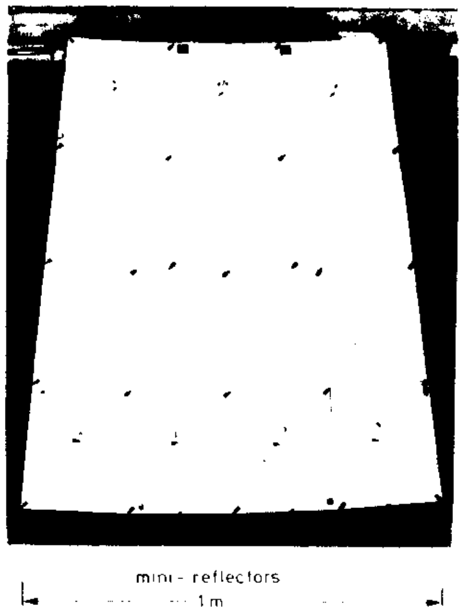


Fig. 5.4: Antenna panel constructed from small elements

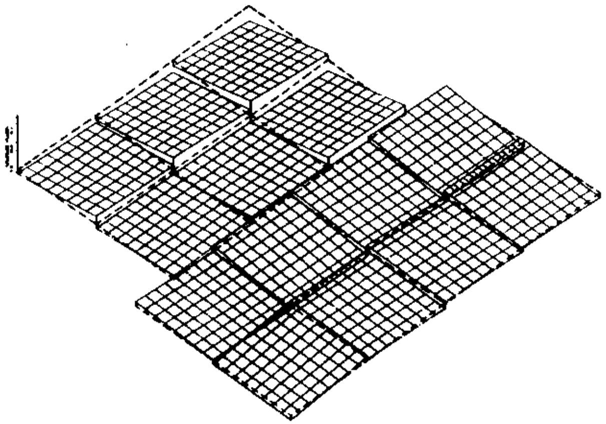

Fig. 5.5: Measured deformation



## 5.3 Experimental stress analysis

Experimental stress analysis is a wide field for the application of holographic interferometry. In this case the method is in competition with the conventional strain gauge technique. However, for the investigation of stress fields holographic interferometry has a lot of advantages.

The deformation behaviour of a pressure vessel, 5 m length and 0.6 m diameter, should be measured under internal water pressure in the area of a bump, fig. 5.6. Conventional methods would require mor than 50 strain gauges, so holographic interferometry was chosen as method. All the equipment was mounted onto the tube, which layed on the ground of the work shop. Although the deformation could be measured, fig. 5.7.

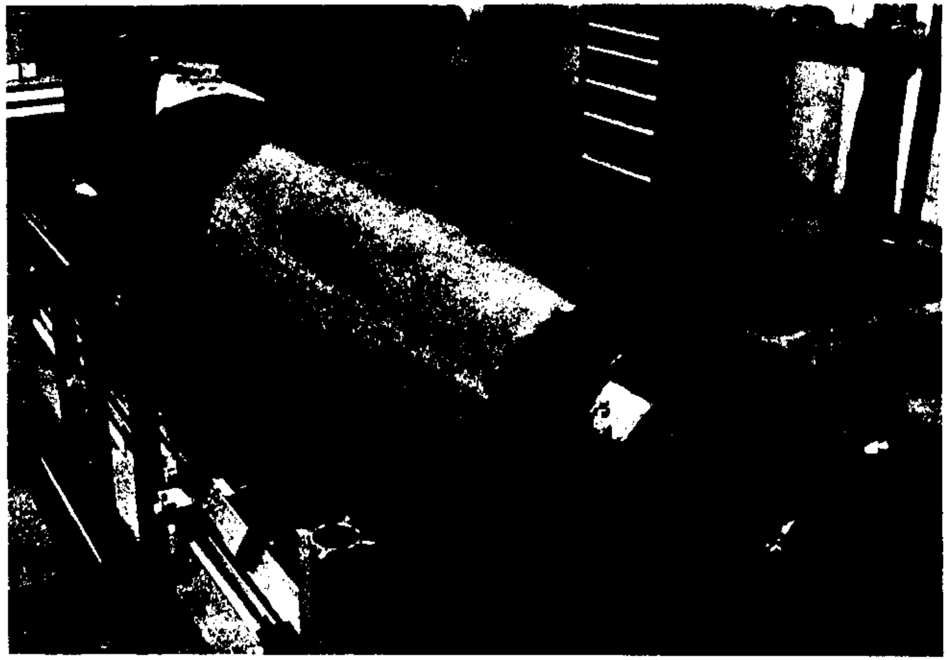

Fig. 5.6: Pressurized water tube

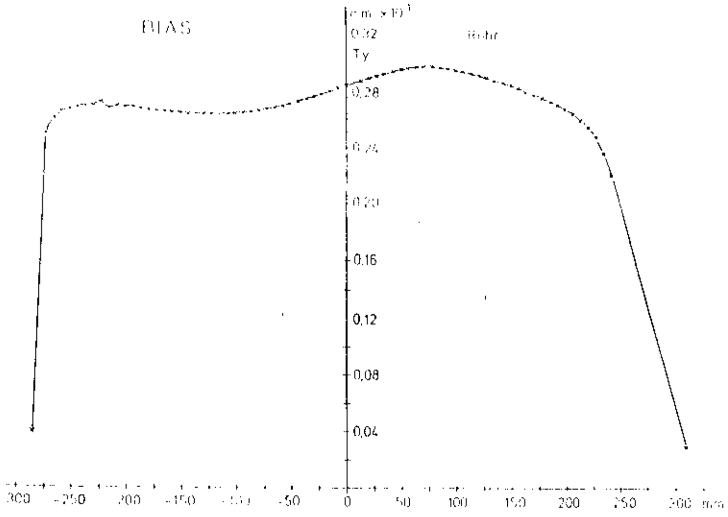


Fig. 5.7: Measured results



# 6. Appendices



## 6.1 References

***Kapitel 1***

/1/ Hecht, E.; Zajac, A.; "Optics"; Addison-Wesley Publ. Co., 1964

/2/ Gabor, D.; "A New Microscopic Principle"; Nature 161, 1948, p. 777 - 778

/3/ Leith, E.N.; Upatnieks, J.; "Reconstructed Wavefronts and Communication Theory"; J. Opt. Soc. Am. 52, 1962, p. 1123 - 1130

/4/ Hariharan, P.; "Optical Holography"; Cambridge Monographs in Physics, Cambridge, 1984

/5/ Tyrer, J.; "Electronic Speckle Pattern Interferometry"; SPIE-Proc. Vol. 604

/6/ Raimann, G.; "Eumig HT-10: Ein TV-Speckle Interferometer und seine praktischen Anwendungen"; Herbstschule '77, Hannover 1977

***Kapitel 4***

/1/ Crostack, H.-A.; " Eine neue Methode zur Auswertung von Interferogrammen"; Vortrag DGZfP, Göttingen, 1976

/2/ Dändliker, R.; "Extrapolation of strain and stress from holographically measured surface displacement"; VDI-Berichte Nr. 313

/3/ Jüptner, W.; "Automatisierte Auswertung holografischer Interferenzmuster mit dem Zeilen-Scan-Verfahren"; DPG/DGaO Frühjahrsschule, Hannover (1978)

/4/ Jüptner, W., Kreis, Th., Kreitlow, H.; "Automatic evaluation of holographic interferograms by reference beam phase shifting"; Proc. SPIE, vol. 398 (1983)

/5/ Kreis, Th., Jüptner, W.; "Digital Processing of Holographic Interference Patterns Using Fourier-Transform Methods"; Proc. IMEKO-Symp. on Laser Applic. in Prec. Measurements, Budapest, Plenum Press Ltd., London 1987

/6/ Dändliker, R.; Ineichen, B.; Mottier, F.M.; "High Resolution Interferometry by Electronic Phase Measurement", Opt. Commun. 9 (4), 413-416, 1973

Table - : Photographic materials for holography

| Type: Plates | Type: Film | Sensitivity Rage | Exposure ($J/m^2$) | Emulsion thickness /um: Plate | Emulsion thickness /um: Film | Resolution $mm^{-1}$ |
|---|---|---|---|---|---|---|
| Agfa-Gevaert (Holotest) | | | | | | |
| 10E56 | 10E56 | Blue-green | $10^{-2}$ | 7 | 5 | 3000 |
| 10E75 | 10E75 | Red | $5x10^{-3}$ | 7 | 5 | 3000 |
| 8E56HD | 8E56HD | Blue-green | $2.5x10^{-1}$ | 7 | 5 | > 3000 |
| 8E75HD | 8E75HD | Red | $10^{-1}$ | 7 | 5 | > 3000 |
| Eastman Kodak | | | | | | |
| 649F | 649F | Panchro | $5x10^{-1}$ | 15 | 6 | > 3000 |
| 120-01/02 | SO-173 | Red | $2x10^{-1}$ | 6 | 6 | > 3000 |
| 125-01/02 | SO-424 | Blue-green | $5x10^{-2}$ | 7 | 3 | 1250 |
| 131-01/02 | SO-253 | Red | $3x10^{-3}$ | 9 | 9 | 1250 |

Table C. Results of Holographic NDT

| Defect Type | Defect Indication | Valuation (Project Leader) | Remarks |
|---|---|---|---|
| Reference | defect free | base fringe system | reference |
| Cuts (1) | local disturbance | hardly detectable | wrong, only guessed |
| Cuts (3) | local disturbance | cut indication | ok, needs training |
| Cuts (5) | local disturbance | good cut indication | ok |
| Knots (1.) | local disturbance | good knot indication | ok |
| Knots (2.) | local disturbance | knot indication | partially ok |
| Miss. band (2) | periodical disturbance | indication missing band | ok |
| Miss. band (3) | periodical disturbance | good indication missing band | ok |
| Miss. band (4) | periodical disturbance | good indication missing band | ok |
| Dry layers (3) | destroyed fringe system | good indication | ok |
| Dry layers (5) | destroyed fringe system | good indication | ok |
| Impact | local disturbance | indication local defect | ok |
| Wrong plastic | lower stiffness | indication material change | ok |
| Wrong plastic | lower stiffness | indication material change | ok |
| Wrong glass | lower stiffness, strength | indication glass change | ok |

Cuts: (i) = number of affected layers, knots: (i) = relative intensity,
Miss. bands: (i) = number of missing bands in one layer, dry layers: (i) = number of layers